Journal of Zhejiang University-SCIENCE B (Biomedicine & Biotechnology) 2023 24(7):587-601
www.jzus.zju.edu.cn; www.springer.com/journal/11585
E-mail: jzus_b@zju.edu.cn

Research Article
https://doi.org/10.1631/jzus.B2200587

Diacylated anthocyanins from purple sweet potato (*Ipomoea batatas* L.) attenuate hyperglycemia and hyperuricemia in mice induced by a high-fructose/high-fat diet

Luhong SHEN[1], Yang YANG[1], Jiuliang ZHANG[1]✉, Lanjie FENG[1], Qing ZHOU[2]✉

[1]*College of Food Science and Technology, Huazhong Agricultural University, Wuhan 430070, China*
[2]*Department of Pharmacy, Wuhan City Central Hospital, Tongji Medical College, Huazhong University of Science and Technology, Wuhan 430014, China*

Abstract: Studies have shown that targeting xanthine oxidase (XO) can be a feasible treatment for fructose-induced hyperuricemia and hyperglycemia. This study aimed to evaluate the dual regulatory effects and molecular mechanisms of diacylated anthocyanins from purple sweet potato (diacylated AF-PSPs) on hyperglycemia and hyperuricemia induced by a high-fructose/high-fat diet. The body weight, organ index, serum biochemical indexes, and liver antioxidant indexes of mice were measured, and the kidneys were observed in pathological sections. The relative expression levels of messenger RNAs (mRNAs) of fructose metabolism pathway enzymes in kidney were detected by fluorescent real-time quantitative polymerase chain (qPCR) reaction technique, and the expression of renal transporter protein and inflammatory factor pathway protein was determined by immunohistochemistry (IHC) technique. Results showed that diacylated AF-PSPs alleviated hyperuricemia in mice, and that this effect might be related to the regulation of liver XO activity, lipid accumulation, and relevant renal transporters. Diacylated AF-PSPs reduced body weight and relieved lipid metabolism disorder, liver lipid accumulation, and liver oxidative stress, thereby enhancing insulin utilization and sensitivity, lowering blood sugar, and reducing hyperglycemia in mice. Also, diacylated AF-PSPs restored mRNA levels related to renal fructose metabolism, and reduced kidney injury and inflammation. This study provided experimental evidence for the mechanisms of dual regulation of blood glucose and uric acid (UA) by diacylated AF-PSPs and their utilization as functional foods in the management of metabolic syndrome.

Key words: Diacylated anthocyanins from purple sweet potato (diacylated AF-PSPs); Hyperglycemia; Hyperuricemia; Metabolism syndrome; Regulation of renal function

1 Introduction

The change toward higher carbohydrate in the human diet increases the risk of hyperglycemia, a chronic metabolic disorder characterized by excess glucose in the circulation (Gowd et al., 2019; Spínola et al., 2019). Also, high-fructose and high-fat diets increase the occurrence of hyperuricemia. The end product of purine nucleoside metabolism is uric acid (UA), and persistently elevated serum UA levels lead to hyperuricemia. About one-third of UA metabolism results from disturbances in purine metabolism due to regular consumption of foods such as fructose, alcoholic beverages, and purine-rich foods. These foods generate excess UA in response to xanthine oxidase (XO) and other enzymes, thereby increasing the risk of hyperuricemia (Yang et al., 2020a).

Many studies have shown that hyperuricemia is closely related to hyperglycemia (Khichar et al., 2017; Yang et al., 2020b). Firstly, hyperuricemia is assumed to increase blood glucose, thus enhancing sodium reabsorption mechanisms. This increases UA reabsorption and finally increases blood UA levels (Adnan et al., 2019). On the other hand, hyperuricemia is also considered as an independent risk factor for diabetes (Krishnan et al., 2012). Increasingly, reports show that

✉ Jiuliang ZHANG, zjl_ljz@mail.hzau.edu.cn
Qing ZHOU, qingz_zqing@aliyun.com
Jiuliang ZHANG, https://orcid.org/0000-0002-1745-846X
Qing ZHOU, https://orcid.org/0009-0000-0761-4572

Received Nov. 20, 2022; Revision accepted Jan. 6, 2023;
Crosschecked Feb. 22, 2023; Published online Apr. 15, 2023

lowering UA may alleviate hyperglycemia to some extent (Nishikawa et al., 2020). Secondly, high-fructose intake may induce hyperglycemia. The metabolism of fructose in the liver leads to high fat production. Elevated free fatty acids and lipid peroxidation inhibit tissue insulin receptors, thus reducing the tissue response to insulin signals and leading to hyperglycemia finally (Nakagawa et al., 2020). The current commercially available therapeutic drugs have certain side effects and are generally not recommended clinically for patients with hyperuricemia and initial hyperglycemia without gout symptoms. Therefore, there is an urgent need to find natural products with fewer side effects to prevent and regulate fructose-induced hyperglycemia combined with hyperuricemia. However, few effective drugs are available to intervene in both diseases, and there is an extreme lack of research reports on related drugs or natural compounds.

Purple sweet potato (*Ipomoea batatas* L.) is considered a functional food due to its abundant content of anthocyanins. The anthocyanin content of purple sweet potato may reach 180 mg/100 g, which is similar to that in berries, but their chemical structures are quite different. Berry anthocyanins are non-acylated small molecule anthocyanins (Kirakosyan et al., 2018). In contrast, the anthocyanins from purple sweet potato (AF-PSPs) are acylated macromolecular forms cyanidin and peonidin, with a single or double acylated locust glycosides attached at the C-3 position and a glucoside attached at the C-5 position. Studies have shown that acylated AF-PSPs are considered a natural phytoconstituent with stable chemical properties and good biological activity, including antioxidant, anti-inflammatory, hypoglycemic, hypolipidemic, hypo-uric acid, and hepatoprotective effects (Wang et al., 2010; Wang et al., 2017; Jokioja et al., 2020). The chemical properties and biological activity of anthocyanins are highly variable depending on their chemical structures, and acylated anthocyanins are more stable in nature than anthocyanins that are not acylated.

Our previous study found that the natural acylated AF-PSPs had a significant dual preventive and intervention effect on hyperglycemia and hyperuricemia, which might provide a valuable research opportunity and material basis for developing natural compounds or dietary interventions (Yang et al., 2020b). Results showed that diacylated AF-PSPs had good XO inhibitory activity in vitro, with the acylated moiety playing an important role. It was also found that diacylated AF-PSPs had a good UA-lowering effect in vivo, and in combination with allopurinol might reduce the oxidative stress and renal damage brought by side effects (Yang et al., 2020a). However, their dual regulatory role in fructose-induced hyperglycemia and hyperuricemia or its molecular mechanism was not yet clear. Whether diacylated AF-PSPs as effective XO inhibitors could alleviate hyperglycemia, and whether their regulatory mechanism was related to XO inhibition, regulation of hepatic metabolic capacity, or promotion of renal metabolism and excretory function deserved further study (Spínola et al., 2019).

In this study we investigated the dual regulatory effect and molecular mechanism of diacylated AF-PSPs on hyperglycemia and hyperuricemia induced by a high-fructose/high-fat diet. The results provide a scientific basis for the prevention and regulation of metabolic syndrome by natural components with a flavonoid structure such as AF-PSPs, also provide a theoretical basis and experimental reference for the application of AF-PSPs as a raw material in high value-added functional foods.

2 Materials and methods

2.1 Chemicals

Allopurinol was purchased from Tokyo Kasei Kogyo Co. (Tokyo, Japan); sodium carboxymethylcellulose was from Sinopharm Chemical Reagent Co. (Shanghai, China); kits for determination of UA, blood urea nitrogen (BUN), creatinine (Cr), total triglyceride (TG), total cholesterol (TC), glucose (Glu), total superoxide dismutase (T-SOD), total malondialdehyde (MDA), reduced glutathione (GSH), total protein, XO, aspartate aminotransferase (AST), and alanine aminotransferase (ALT) were from the Nanjing Jiancheng Institute of Biological Engineering (Nanjing, China). A mouse insulin enzyme-linked immunosorbent assay (ELISA) kit was purchased from Shanghai Thermo Fisher Scientific Co. (Shanghai, China); rabbit polyclonal antibodies sodium-dependent glucose transporters 2 (SGLT2), glucose transporter 2 (GLUT2), GLUT5, GLUT9, urate transporter 1 (URAT1), mouse monoclonal antibodies nuclear factor-κB p65 (NF-κB p65), interleukin-6 (IL-6), and tumor necrosis factor-α (TNF-α) were from the Wuhan Sanying Biotechnology Co. (Wuhan, China).

Rabbit polyclonal antibody IL-1β was purchased from Affinity Biosciences (Melbourne, Australia). All other regular reagents were of analytical grade and purchased from Sinopharm Chemical Reagent Co., Ltd.

2.2 Preparation of diacylated AF-PSPs

Anthocyanin extraction was performed using an established method (Luo et al., 2018; Zhang JT et al., 2019). A total of 100 g purple sweet potato powder (*Ipomoea batatas* L. cultivar Eshu No. 8) was mixed with 1000 mL of extraction solution (anhydrous ethanol: 0.1 mol/L HCl=60: 40, volume ratio), ultrasonic extraction with Ultrasonic Cleaner (Shanghai Kerr Instruments Co., Shanghai, China) at 60 ℃ for 30 min and centrifuged at 4000 r/min for 10 min. The supernatant was rotary-evaporated and extracted with a triple volume of ethyl acetate, and then the crude anthocyanin extract was obtained by vacuum freeze-drying.

The crude anthocyanin extract was dissolved, filtered, and loaded on the column proportionally. The resin was rinsed continuously with five bed volume (BV) of 0.1% (volume fraction) HCl after each sample was completely adsorbed. Then, 4 BV of eluent (anhydrous ethanol:citric acid-disodium hydrogen phosphate (pH 3.0)=70:30) was added for elution. The eluent flow rate was controlled at 4 mL/min. The first purified anthocyanin extract was obtained by rotary evaporation concentration and vacuum freeze-drying, and then dissolved, filtered, and loaded again on the column. The column was rinsed in turn with double-distilled water, 5 BV of double-distilled water containing 0.1% (volume fraction) trifluoroacetic acid (TFA), and 5 BV of 10% (volume fraction) methanolic water containing 0.1% (volume fraction) TFA. Samples obtained by elution of 30% and 40% methanolic aqueous solutions containing 0.1% (volume fraction) TFA were collected separately, concentrated by rotary evaporation, and freeze-dried under vacuum. These extracts, named monoacylated AF-PSPs and diacylated AF-PSPs, respectively, were then placed in sealed aluminum foil bags and stored at −20 ℃.

The total anthocyanin content was measured by the pH difference method using peonidin-3-caffeoyl-feruloyl sophoroside-5-glucoside as a standard sample. Later, animal experiments included diacylated AF-PSPs as a test sample. The total anthocyanin content of diacylated AF-PSPs was (509.81±1.21) mg/g peonidin-3-caffeoyl-feruloyl sophoroside-5-glucoside equivalent. The monomeric structures of the purified fragments of purple sweet potato are shown in Table S1.

2.3 Animals

A total of 50 specific pathogen free (SPF)-grade male Kun-Ming strain mice ((20±2) g, aged four weeks) were purchased from the Experimental Animal Center of Huazhong Agricultural University (Wuhan, China). All animals were kept under a 12-h light/12-h dark cycle. Both basic feed and high-fat feed (fat energy accounted for 45%) were purchased from Wuhan Wanqian Jiaxing Biotechnology Co., Ltd. (Wuhan, China). Crystalline fructose was purchased from the Xiwang Sugar Co., Ltd. (Zouping, China).

2.4 Establishment of mice model of hyperuricemia and hyperglycemia induced by a high-fructose/high-fat diet

The experimental mice were randomly divided into five groups: the normal control group (NC), the model group (Model), positive group (AP), low-dose diacylated AF-PSPs group (L-DiAF), and high-dose diacylated AF-PSPs group (H-DiAF). Each group contained ten mice. The whole experimental period was nine weeks (Fig. S1). Feeding and drinking conditions were set as follows: the NC group was on the standard basic feed and standard water; other groups were on the same intake of high-fat feed and 0.2 g/mL fructose solution from bottles. Each group was given gavage treatment based on their body weight from four weeks onwards. The gavage sample conditions were as follows: the NC and Model groups were given 10 mL/kg body weight (BW) of double distilled water, the AP group was given 5 mg/kg BW of allopurinol (dissolved in 0.5% (volume fraction) sodium carboxymethyl cellulose (CMC-Na), and the L-DiAF and H-DiAP groups were given diacylated AF-PSPs solution at 25 and 50 mg/kg BW, respectively. The high-fat feed contained 68.8% (mass fraction, the same as below) normal diet, 15.0% sucrose, 10.0% lard, 5.0% custard powder, 1.0% cholesterol, and 0.2% choline bitartrate. The high-fat feed contained 45% fat, 20% protein, and 35% carbohydrate, with 4.73 kcal/g in each diet. The basic feed contained 10% fat, 20% protein, and 70% carbohydrate, with 3.85 kcal/g in each diet.

2.5 Measurement of indicators

2.5.1 Glucose tolerance test

After a 4-week gavage, the mice were fasted for 16 h with the 20% fructose solution replaced by double distilled water. Each group was then given 2 g/kg BW glucose solution. Tail vein blood was collected at 0, 30, 60, 90, and 120 min, and the blood glucose level was measured with a Roche blood glucose meter (MY-20 ACCU-CHEK Active, Roche Diagnostic Products Co., Shanghai, China).

2.5.2 Sample collection and storage

The mice were given two days to recover after the glucose tolerance test, and then treated with water and fasting for 12 h. After anesthetized using Uratan (Beijing Chreagen Biotechnology Co., Ltd., Beijing, China), their eyeballs were removed to collect blood. The blood samples were centrifuged at 3000*g* (high-speed frozen centrifuge, Beckman Coulter Co., CA, USA) for 10 min at 4 ℃ after naturally clotting for 1 h, and then the supernatant was sub-packaged and stored at −80 ℃ in an ultra-low temperature refrigerator (Shanghai Thermo Fisher Scientific Co.). Experimental mice were sacrificed by cervical dislocation after blood sampling, and their liver and kidney tissues were dissected and extracted. Their organs were rinsed in 4 ℃ pre-cooled physiological saline, dried with filter paper, and weighed. An organ index was calculated based on the following formulas:

$$\text{Liver index}=\text{liver weight (g)}\times 100/\text{mouse BW (g)}, \quad (1)$$

$$\text{Kidney index}=\text{kidney weight (g)}\times 100/\text{mouse BW (g)}. \quad (2)$$

2.5.3 Determination of serum biochemical indicators

Test kits for Glu, UA, Cr, BUN, TG, TC, ALT, and AST, and a mouse insulin ELISA kit were used after the samples were naturally thawed at 4 ℃. The determination process was carried out in accordance with the operating instructions of the relevant kit. Homeostasis model assessment of insulin resistance (HOMA-IR) was calculated according to the following formula:

$$\text{HOMA-IR}=\text{fasting blood glucose (mmol/L)}\times \text{serum insulin value (mU/L)}/22.5. \quad (3)$$

2.5.4 Determination of biochemical indexes of liver tissue

Normal saline pre-cooled to 4 ℃ was added to each mouse liver tissue sample and homogenized in a tissue homogenizer (Shanghai Jingxin Industrial Development Co., Shanghai, China) under ice bath conditions. The homogenate was centrifuged at 3500*g* for 10 min at 4 ℃. The supernatant was taken as 10% (mass fraction) liver tissue homogenate and sub-packaged and stored at −20 ℃ for testing to avoid repeated freezing and thawing. Test kits for total protein, TG, TC, XO, MDA, GSH, and T-SOD activity determination were used to measure the relevant liver homogenate indexes. The determination process was carried out in accordance with the operating instructions of the relevant kit.

2.5.5 Pathological examination of kidney tissue

Fresh kidney tissue samples were selected randomly from experimental mice and placed in 4% (volume fraction) paraformaldehyde solution for fixation with at least 24 h. Ultimate samples were scanned with CaseViewer 3.3 software (https://www.3dhistech.com) at 400× magnification after dehydration with different concentration gradients of ethanol, washing with xylene, embedding in paraffin wax, conventional sectioning, dewaxing, and hematoxylin-eosin (HE) staining.

2.5.6 Real-time fluorescent polymerase chain reaction analyses of enzymes related to fructose metabolism in the kidney

A total of 100 mg of tissue with 1 mL of Trizol extraction reagent was added to a sterilized and pre-cooled homogenization tube and ground thoroughly. After centrifugation at 12 000 r/min for 10 min, the supernatant was fixed with 250 μL trichloromethane, left to stand for 3 min, and then centrifuged at 12 000 r/min using a tabletop high-speed frozen microcentrifuge (Beijing Dalong Xingchuang Experimental Instrument Co., Beijing, China) for 10 min at 4 ℃. Then, 400 μL supernatant was transferred to a new centrifuge tube, and 80% (volume fraction) of isopropanol was added, left for 15 min at −20 ℃, and then centrifuged at 12 000 r/min for 10 min at 4 ℃. The white precipitate at the bottom of the tube was RNA. The liquid was aspirated off, and the centrifuge tube was placed on an ultra-clean table to dry for 3 min. A total of

15 μL of RNA-free water was added to dissolve the RNA and the solution was incubated for 5 min at 55 ℃. Nanodrop 2000 (Thermo Fisher Scientific Co., Shanghai, China) was used to detect the RNA concentration and purity using 2.5 μL of RNA solution, and the final concentration was controlled at 100–500 ng/μL. The sequences of primers used are shown in Table S2.

2.5.7 Immunohistochemistry (IHC) analyses of transport proteins and inflammation-related proteins in kidney tissue

Wax-embedded fixed kidney tissues (4-μm thickness) were treated with xylene and ethanol, and the paraffin was removed and dehydrated. Citrate buffer (10 mmol/L, pH 6.0) was used for antigen retrieval in two 5-min microwave treatments. The sections were incubated with 3% (volume fraction) hydrogen peroxide-methanol for 10 min, 10% (volume fraction) serum for 30 min at room temperature, and then with antibody overnight at 4 ℃. The sections were incubated with the secondary antibody for 30 min at room temperature, and then incubated with horseradish peroxidase-labeled streptavidin at 37 ℃ for 30 min. The observation of protein expression used 30 mg/mL 3,3'-diaminobenzidine tetrahydrochloride containing 0.03% (volume fraction) hydrogen peroxide. All slices were scanned and images were recorded with CaseViewer 3.3 software. The immunohistochemical positive area was quantitatively analyzed using ImageJ software (https://imagej.net) based on ten fields of view in each slice. Related reagents were purchased from Sinopharm Chemical Reagent Co. (Shanghai, China).

2.5.8 Data analysis and processing

Results are expressed as mean±standard deviation (SD). SPSS® 22.0 one-way analysis of variance (ANOVA) and Duncan's multiple range test (DMRT) were used to analyze the significance of data. Data were judged to be statistically significant when P was <0.05. Origin 9.0 software (https://www.originsoftware.net) was used to draw corresponding charts.

3 Results and discussion

3.1 Recovery of liver and kidney indexes by diacylated AF-PSPs

After eight weeks of feeding, the body weight of the Model group showed a significant increase compared with the NC group, while other groups showed no significant difference from NC (Table 1). Also, the body weight in the H-DiAF group decreased significantly compared to that of the Model group. This indicated that the 8-week high-fructose/high-fat diet

Table 1 Effects of diacylated AF-PSPs on body weight, organ indexes, serum biomarkers, and liver oxidative stress biomarkers of high-fructose/high-fat diet-fed mice

Group	Body weight (g)	Organ index				Serum biomarker	
		Liver weight (g)	Liver index (%)	Kidney weight (g)	Kidney index (%)	BUN (mmol/L)	Cr (μmol/L)
NC	41.80±3.57^{b}	1.86±0.26^{b}	4.44±0.98^{a}	0.67±0.09^{a}	1.59±0.25^{a}	6.59±0.38^{b}	11.61±2.64^{b}
Model	46.64±4.22^{a}	2.09±0.22^{a}	4.62±0.69^{a}	0.58±0.06^{b}	1.25±0.15^{b}	8.47±0.75^{a}	16.32±1.47^{a}
AP	43.50±3.23^{ab}	1.92±0.07^{b}	4.45±0.44^{a}	0.62±0.05^{a}	1.42±0.14^{a}	6.99±1.04^{b}	12.01±4.42^{b}
L-DiAF	43.42±2.55^{ab}	1.94±0.17^{ab}	4.50±0.53^{a}	0.63±0.06^{a}	1.44±0.15^{a}	6.94±0.56^{b}	12.51±2.07^{ab}
H-DiAF	42.66±2.19^{b}	1.89±0.42^{b}	4.44±1.09^{a}	0.64±0.08^{a}	1.50±0.21^{a}	7.08±0.79^{b}	11.60±3.48^{b}

Group	Serum biomarker				Liver oxidative stress biomarker		
	TC (mmol/L)	TG (mmol/L)	ALT (U/L)	AST (U/L)	T-SOD (U/mg prot)	MDA (nmol/mg prot)	GSH (μmol/L)
NC	1.57±0.21^{b}	0.60±0.16^{c}	7.93±1.91^{a}	12.20±2.94^{a}	406.04±69.96^{c}	2.10±0.67^{b}	19.84±6.65^{a}
Model	2.17±0.51^{a}	1.20±0.36^{a}	7.60±1.83^{a}	11.11±2.45^{a}	312.48±31.11^{a}	3.29±0.95^{a}	13.70±1.76^{b}
AP	2.04±0.59^{ab}	0.80±0.13^{b}	7.79±1.07^{a}	10.59±3.59^{a}	323.69±62.79^{ab}	2.67±0.50^{ab}	15.10±3.50^{b}
L-DiAF	1.86±0.20^{ab}	0.74±0.10^{bc}	8.40±1.69^{a}	10.67±2.90^{a}	365.18±54.75^{abc}	2.38±0.62^{b}	14.79±3.04^{b}
H-DiAF	1.61±0.42^{b}	0.75±0.12^{bc}	8.23±1.36^{a}	11.69±2.79^{a}	376.08±28.68^{bc}	2.18±0.93^{b}	16.48±2.51^{ab}

Values are expressed as mean±standard deviation (SD), n=10. Different letters indicate significant differences between groups (Duncan's test, P<0.05). AF-PSPs: anthocyanins from purple sweet potato; NC: normal control; AP: positive; L-DiAF: low-dose diacylated AF-PSPs; H-DiAF: high-dose diacylated AF-PSPs; BUN: blood urea nitrogen; Cr: creatinine; TC: total cholesterol; TG: triglyceride; ALT: alanine aminotransferase; AST: aspartate aminotransferase; T-SOD: total superoxide dismutase; MDA: malondialdehyde; GSH: glutathione; prot: protein.

caused weight gain and some degree of obesity. This might have been related to the large amount of fat produced by fructose metabolism in liver, coupled with the accumulation of body fat due to the high-fat intake. After gavage of 50 mg/kg BW diacylated AF-PSPs for four weeks, body weight returned to normal values. The reduction in body weight was better than that achieved by the UA-lowering drug allopurinol.

For liver weight, the Model group was significantly heavier than the NC group, while the liver weights of the AP and H-DiAF groups were reduced to the normal control level. No significant differences were found between the liver indexes of the mice in each group. In other studies, mice fed with a high-fructose/high-fat diet showed significant increases in liver weight and index, indicating some degree of liver fat accumulation, but some flavonoids were able to mitigate (Zhang ZC et al., 2019; Lu et al., 2021). Allopurinol and 50 mg/kg BW diacylated AF-PSPs reduced kidney fat accumulation and thus reduced kidney weight. The absence of significant changes in liver index in mice fed with high-fructose/high-fat may suggest that diacylated AF-PSPs did not cause significant abnormal toxic damage to the mouse liver during gavage. In addition, the kidney weight and index were clearly lower in the Model group than in the NC group, and both allopurinol and diacylated AF-PSPs by gavage restored the liver weight and index to the normal level. A high-fructose/high-fat diet might induce kidney atrophy as a manifestation of renal inflammation and chronic kidney disease (van Hung et al., 2019; Thongnak et al., 2020). In contrast, diacylated AF-PSPs restored the kidneys of the mice and might help to reduce renal inflammation.

3.2 Improvement of blood glucose regulation by diacylated AF-PSPs

Fig. 1 showed the changes of blood glucose values and area under the curve (AUC) in blood glucose from 0 to 120 min after gavage of glucose. Each group of mice reached its peak at 30 min after gavage. Mice in the Model group had a faster rise in blood glucose, which was significantly higher than that of the NC group. The peaks of blood glucose levels of mice in the AP and H-DiAF groups were significantly lower than normal levels. Mice in the Model group had significantly higher AUC values than those in the NC group. The AUC values of mice in the AP and H-DiAF groups were significantly lower than those of the Model group, but not significantly different from those of the NC group.

Results showed that after eight weeks of the high-fructose/high-fat diet, the mice exhibited an impaired glucose tolerance state with elevated peak glucose level and AUC, and a decreased ability to regulate blood glucose. This indicates the possibility of developing type 2 diabetes and persistently high blood glucose levels (Lu et al., 2021). Gavage treatment with allopurinol and 50 mg/kg BW diacylated AF-PSPs significantly improved the regulation of blood glucose and reduced the possibility of further development of type 2 diabetes. This suggests that XO inhibitors might have a modulatory effect on hyperglycemia induced by a high-fructose/high-fat diet (Ng et al., 2020).

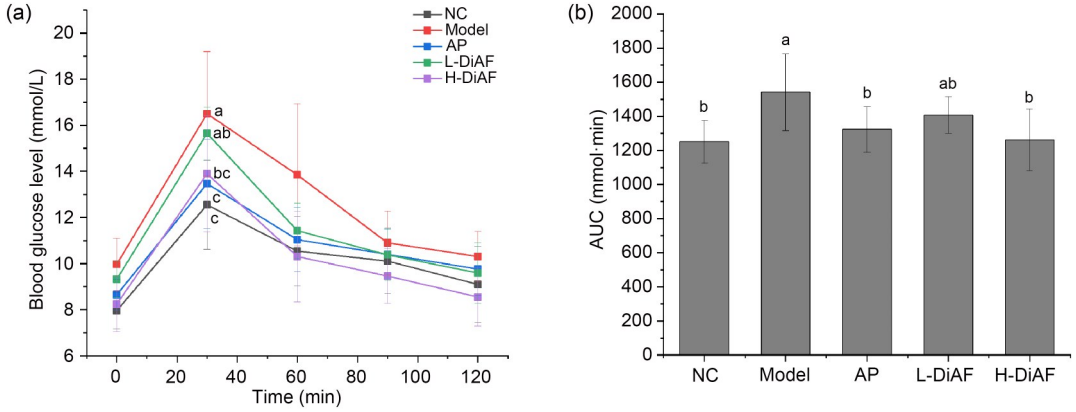

Fig. 1 Effects of diacylated AF-PSPs on glucose tolerance (a) and the corresponding AUC (b) of high-fructose/high-fat diet-fed mice. Values are expressed as mean±standard deviation (SD), *n*=10. Different letters indicate significant differences between groups (*P*<0.05). AF-PSPs: anthocyanins from purple sweet potato; NC: normal control; AP: positive; L-DiAF: low-dose diacylated AF-PSPs; H-DiAF: high-dose diacylated AF-PSPs; AUC: area under the curve.

3.3 Effects of diacylated AF-PSPs on UA and serum insulin

HOMA-IR is one of the indicators used to evaluate the insulin level in individuals, and the evaluations of fasting blood glucose, insulin, and HOMA-IR levels help to understand the condition of organism. Figs. 2a–2d showed that there was a significant increase in blood UA values after eight weeks of the high-fructose/high-fat diet. Fasting blood glucose values in the AP and H-DiAF groups were significantly lower than those of the Model group. The high-fructose/high-fat diet resulted in impaired fasting glucose levels in the mice, which were somewhat improved by gavage of allopurinol and 50 mg/kg BW of diacylated AF-PSPs. After eight weeks of the high-fructose/high-diet, the HOMA-IR values of the NC group were less than 1, whereas those of the mice in the Model group were significantly elevated above 1. The insulin levels of the mice in the L-DiAF and H-DiAF groups returned to the levels of the NC group, and the HOMA-IR levels of the mice in the H-DiAF group returned to a level less than 1. The reduced ability to regulate blood glucose and significantly increased blood UA values in the Model group indicated that the experiment was successful in establishing a hyperuricemia and hyperglycemia mouse model induced by a high-fructose/high-fat diet, which is consistent with the results reported in some studies (Adouni et al., 2018; Seo et al., 2020).

Since hyperuricemia and hyperglycemia are considered risk factors for the development of chronic kidney disease (Johnson et al., 2013; Zhang et al., 2015), this experiment measured BUN and Cr to characterize the effects on kidney function in the mice. Table 1 showed the effect of diacylated AF-PSPs on biochemical indexes characterizing renal function in the serum of the mice. The clearance of BUN and Cr in the Model group showed a decreasing trend. This indicates a decrease in the glomerular filtration rate and in effective kidney units, causing damage to the renal parenchyma of the mice. Diacylated AF-PSPs at 25 and 50 mg/kg BW effectively reduced the serum levels of BUN and Cr in the mice and restored normal kidney function. The modulating effect of diacylated AF-PSPs on kidney function might be related to its ability of reducing UA levels and hypoglycemic effects.

As shown in Figs.2f and 2g, the levels of serum TC and TG in the H-DiAF group were significantly

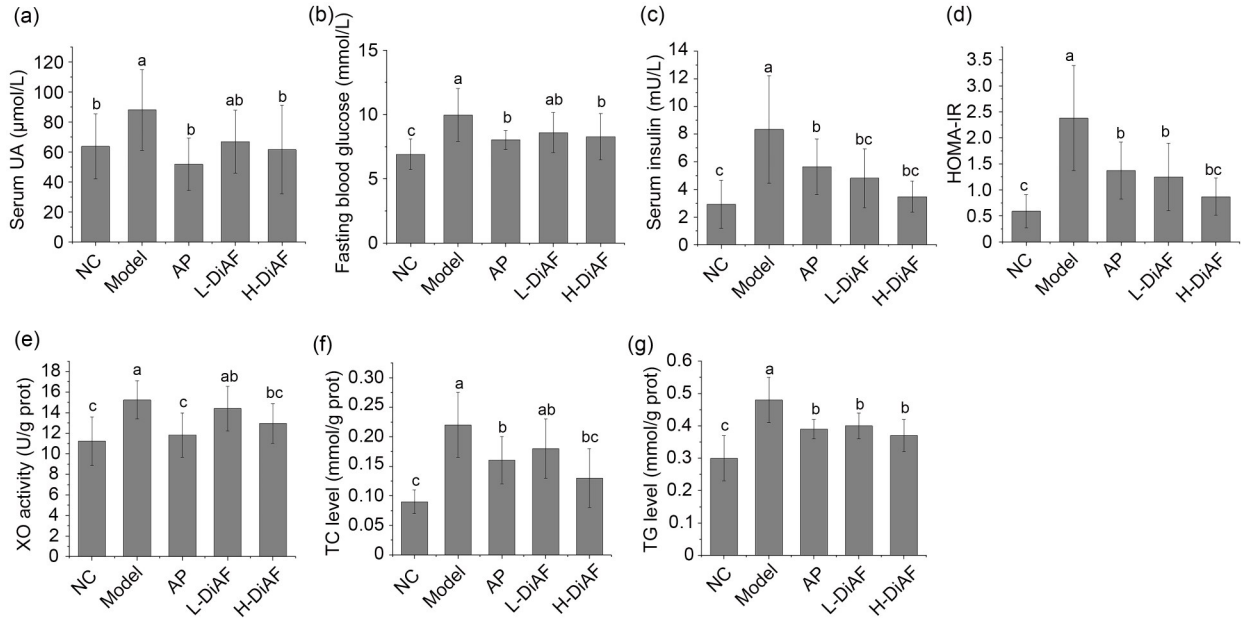

Fig. 2 Effects of diacylated AF-PSPs on serum UA (a), fasting blood glucose (b), serum insulin (c), HOMA-IR (d), liver XO activity (e), TC (f), and TG (g) levels of high-fructose/high-fat diet-fed mice. Values are expressed as mean±standard deviation (SD), *n*=10. Different letters indicate significant differences between groups (*P*<0.05). AF-PSPs: anthocyanins from purple sweet potato; UA: uric acid; HOMA-IR: homeostasis model assessment of insulin resistance; XO: xanthine oxidase; TC: total cholesterol; TG: triglyceride; NC: normal control; AP: positive; L-DiAF: low-dose diacylated AF-PSPs; H-DiAF: high-dose diacylated AF-PSPs; prot: protein.

decreased to normal levels (P<0.05), while only the TG level showed a decrease in the AP and L-DiAF groups (Table 1). The high-fructose/high-fat diet induced not only hyperuricemic and hyperglycemic symptoms, but also some hyperlipidemia and hypercholesterolemia. The hyperlipidemia and hypercholesterolemia were relieved to different degrees by intervention with different doses of diacylated AF-PSPs. The 25 mg/kg BW diacylated AF-PSPs had a moderating effect on lipid metabolism, while 50 mg/kg BW was better than allopurinol in improving the total serum cholesterol in the mice. This reflects the advantages of diacylated AF-PSPs as a multi-targeted natural product. Moreover, it appeared that the gavage of diacylated AF-PSPs did not cause any functional disorder or lesion in the liver.

3.4 Improvement of abnormal UA metabolism by diacylated AF-PSPs

XO is a key enzyme in the hepatic synthesis pathway of UA and an important target for treatment of hyperuricemia as well as the regulation of abnormal UA metabolism (Ma et al., 2019). As shown in Fig. 2e, the liver XO enzyme activity in the Model group was significantly higher than that of the NC group, indicating that the high-fructose feeding of mice induced an increase in liver XO enzyme activity, thereby promoting UA synthesis and causing hyperuricemia. After 4-week intervention with allopurinol and 50 mg/kg BW diacylated AF-PSPs, XO enzyme activity in the mouse liver was significantly inhibited. This indicated that diacylated AF-PSPs, as an effective XO inhibitor, reduced hepatic UA synthesis and thus improved the abnormal UA metabolism caused by the high-fructose intake. This is consistent with the results of previous laboratory study (Zhang ZC et al., 2019). Therefore, the modulatory effect of diacylated AF-PSPs on hyperuricemia could be partially attributed to its inhibition of XO enzyme activity.

To further investigate the effect of diacylated AF-PSPs on lipid accumulation in the mouse liver, the TC and TG contents in the liver were measured. The Model group showed a significant increase compared with the NC group, indicating that the high-fructose/high-fat diet induced liver fat accumulation in mice. Diacylated AF-PSPs at 25 mg/kg BW reduced only the total TG level in the liver. Its ability to regulate the TC level in the liver was limited. These results were generally consistent with the changes in serum TC and total TG. The ability of diacylated AF-PSPs to alleviate a nonalcoholic fatty liver in mice might be partly related to the reduction of blood UA and the normal entry of citric acid into the tricarboxylic acid cycle, thereby regulating lipid synthesis (Zhang et al., 2015; Andres-Hernando et al., 2017; Masarone et al., 2018).

The rapid metabolism of fructose in the liver generates large amounts of reactive oxygen species (ROS) due to a high-fructose/high-fat diet, inducing the development of high glucose and UA levels and liver fat accumulation in mice (Hu et al., 2012; Yang et al., 2020a). Thus, in this experiment, T-SOD activity and MDA and GSH contents were used to characterize the oxidative stress status of the liver. The MDA content in liver of mice in the Model group increased significantly, while the T-SOD activity and GSH content both decreased (Table 1). The high-fructose/high-fat diet induced an increase in hepatic lipid peroxidation and a decrease in the ability of liver to scavenge oxygen free radicals, indicating a decrease in the antioxidant capacity of the liver and a certain degree of oxidative damage to the liver cells. Note that there were no significant differences in the indexes of the AP mice compared to those in the Model group, indicating that allopurinol did not significantly improve the oxidative stress in the mice livers. The 50 mg/kg BW of diacylated AF-PSPs intervention significantly increased liver T-SOD activity and decreased the MDA content compared to the Model group. However, there was no significant difference in GSH content, while 25 mg/kg BW of diacylated AF-PSPs gavage treatment significantly decreased only the liver MDA content of mice. The antioxidant effect of diacylated AF-PSPs on mice livers might be related to its effects of reducing UA production and regulating hepatic lipid metabolism, as well as its effect as an antioxidant substance.

3.5 Effects of diacylated AF-PSPs on reduction of renal damage in mice with hyperuricemia and hyperglycemia

Since the serum indexes suggested renal dysfunction in the mice, HE staining was further used for pathological examination of the kidney (Fig. 3). The glomerular basement and thylakoid membranes of the Model group mice were found to be significantly thickened, and the renal interstitium showed obvious

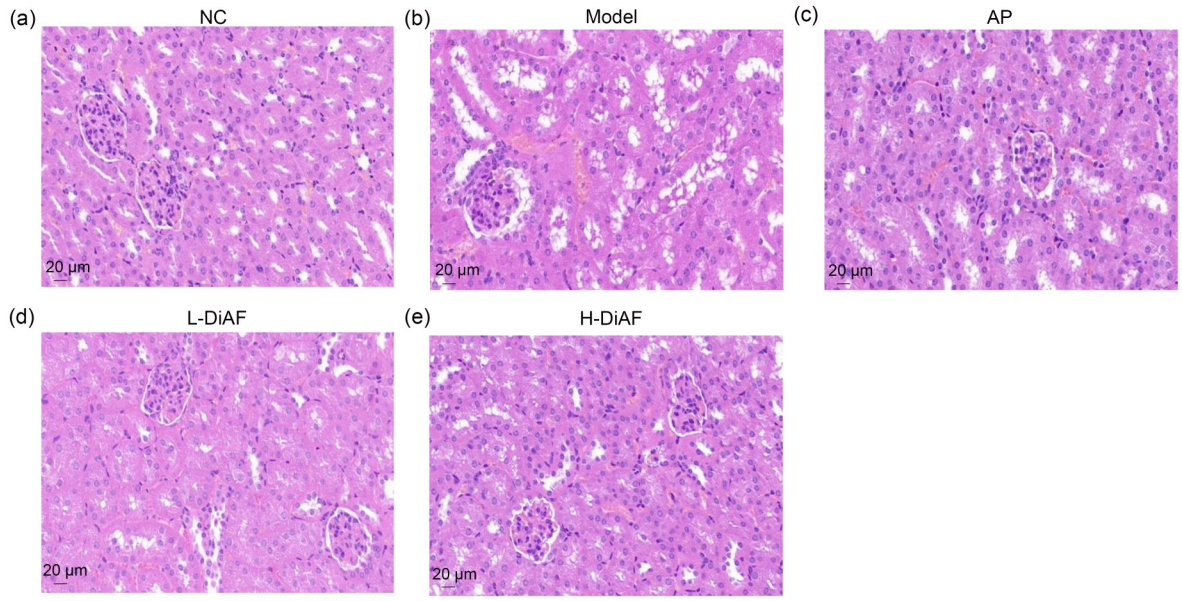

Fig. 3 HE staining of mice renal tissues in the NC (a), Model (b), AP (c), L-DiAF (d), and H-DiAF (e) groups. HE: hematoxylin-eosin; NC: normal control; AP: positive; L-DiAF: low-dose diacylated anthocyanins from purple sweet potato (AF-PSPs); H-DiAF: high-dose diacylated AF-PSPs.

inflammatory cell infiltration. Moreover, there were some changes in renal tubular morphology, including vacuolar degeneration of proximal tubular cells and swelling and enlargement of renal tubular epithelial cells, suggesting tubular injury. The high-fructose/high-fat diet induced renal pathological changes in the mice and caused some degree of renal injury, which might have been related to the stress on the kidney caused by the elevation of blood UA and blood glucose. In contrast, after allopurinol gavage treatment, the histomorphological structure of the kidney was restored to some extent, but thickening of the glomerular basement and thylakoid membranes was still observed.

When fed a high-fructose/high-fat diet for four weeks, the kidneys of the mice might have been affected. Further allopurinol intervention in high-fructose/high-fat diet-fed mice for the following four weeks reduced serum UA, glucose, Cr, and BUN levels, and also restored renal indexes and function. However, it is possible that allopurinol treatment alone could not completely reverse the damage already done to the kidneys of the mice, due to the burden on the kidneys from allopurinol metabolism and excretion in the kidneys (Zhang ZC et al., 2019). The changes in the serum indicators of renal function might have been related to the presence of some degree of renal function compensation. When mice were intervened with diacylated AF-PSPs, renal injury was improved at either dose. Compared with the Model group, the thicknesses of the glomerular basement membrane and thylakoid matrix were significantly reduced following either 25 or 50 mg/kg BW of diacylated AF-PSPs. The morphological structure of the glomeruli was restored, the infiltration of inflammatory cells in the renal interstitium was significantly reduced, the vacuolar degeneration of proximal tubules and swelling of tubular epithelial cells were suppressed, and the tubular cells were closely arranged and maintained a normal morphological structure. We therefore hypothesized that diacylated AF-PSPs could reduce the renal damage in mice associated with hyperuricemia and hyperglycemia, and thus interfere with the process of chronic kidney disease induced by an improper diet. This might be related to its anti-inflammatory and antioxidant activity.

3.6 Restoration of normal expression levels of key enzymes in glucose metabolism by diacylated AF-PSPs

We investigated the effect of diacylated AF-PSPs on the messenger RNA (mRNA) expression levels of fructokinase (*FK*), aldolase B (*AldoB*), aconitase 2 (*Aco2*), and glucose-6-phosphatase (*G6Pase*) in the kidneys of mice fed with a high-fructose/high-fat diet

to demonstrate the effect of its intervention on renal fructose metabolism. Results indirectly indicated that the expression of renal *FK* and *AldoB* might increase while that of *Aco2* and *G6Pase* might decrease (Fig. 4). This might be a result of increased urinary fructose reabsorption and disturbed renal fructose metabolism due to the high-fructose intake. The increase in fructose substrate stimulated the expression of *FK*, which accelerates the phosphorylation of fructose and produces substrates to further induce increased *AldoB* expression (Zhang et al., 2014). On the other hand, the expression of *G6Pase* in the kidney of the Model group showed a decreasing trend. Fructose metabolism consumes a large amount of adenosine triphosphate (ATP) and produces hyperinsulinemia unfavorable to the gluconeogenesis process, which might also lead to the accumulation of lactic acid and lipids (Zhang ZC et al., 2019).

After allopurinol treatment, the mRNA levels of *AldoB*, *Aco2*, and *G6Pase* in the kidneys of mice were restored to normal levels, while the mRNA level of *FK* was not remarkably different to that of the Model group. This suggests that allopurinol could positively regulate the expression of *Aco2* and *G6Pase*, and negatively regulate the expression of *AldoB*. This may have restored the tricarboxylic acid cycle and gluconeogenesis to normal. This might be related the effect of allopurinol on lowering UA and improving blood glucose regulation, but the expression of *FK* as a key target was not significantly affected by the treatment of lowering UA alone. In contrast, intervention with diacylated AF-PSPs at 50 mg/kg BW significantly reduced the mRNA levels of *FK* and *AldoB*, and increased the levels of *Aco2* and *G6Pase* in the mice kidneys compared with the Model group. This indicated that a high-dose of diacylated AF-PSPs could restore the expression levels of *FK*, *AldoB*, *Aco2*, and *G6Pase* to normal, reduce fructose phosphorylation, revert the tricarboxylic acid cycle and gluconeogenesis, and reduce the "Warburg effect" of lipid and lactate accumulation, thus relieving the kidney damage caused by high-fructose intake. Low-dose diacylated AF-PSPs also had a moderating effect on the expression of fructose metabolism-related enzymes in the

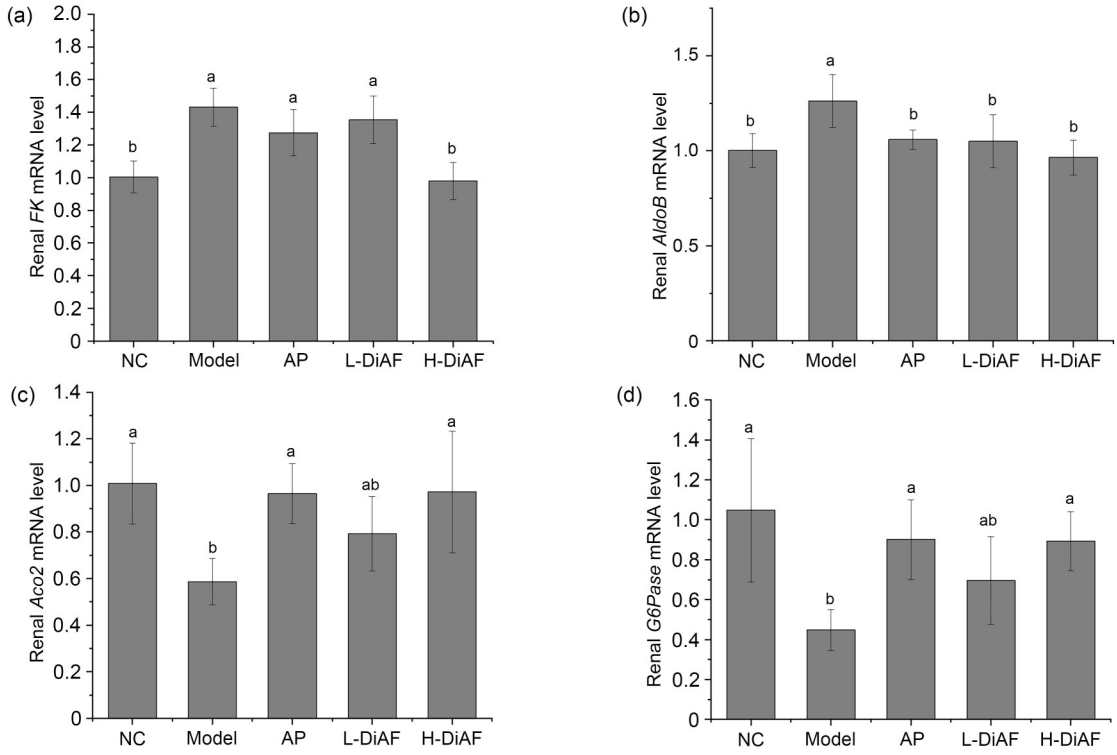

Fig. 4 Effects of diacylated AF-PSPs on renal *FK* (a), *AldoB* (b), *Aco2* (c), and *G6Pase* (d) mRNA expression levels of high-fructose/high-fat diet-fed mice. Values are expressed as mean±standard deviation (SD), *n*=10. Different letters marked above the bar indicate significant differences (*P*<0.05). AF-PSPs: anthocyanins from purple sweet potato; *FK*: fructokinase; *AldoB*: aldolase B; *Aco2*: aconitase 2; *G6Pase*: glucose-6-phosphatase; mRNA: messenger RNA; NC: normal control; AP: positive; L-DiAF: low-dose diacylated AF-PSPs; H-DiAF: high-dose diacylated AF-PSPs.

mice, but the effect was weaker than those of allopurinol and high-dose diacylated AF-PSPs. Knockdown of *FK* or inhibition of *FK* expression in mice can alleviate inflammation and injury in liver and kidney tissues brought about by fructose metabolism. *FK* is a key target in diseases caused by fructose metabolism, and the combination of *FK* inhibitors and UA-lowering therapy might be an appropriate treatment for liver and kidney diseases (Vilà et al., 2011; Zhang et al., 2014). The ability of diacylated AF-PSPs to lower UA and blood glucose might be an influential factor in its ability to regulate renal *AldoB*, *Aco2*, and *G6Pase* expression levels and thus inhibit fructose hypermetabolism.

3.7 Inhibition of renal inflammatory response of kidneys in mice with metabolic syndrome by diacylated AF-PSPs

Mouse kidney IHC experiments were performed to investigate the expression levels of purple sweet potato extract on renal UA, fructose, glucose reabsorption transporter protein, and inflammation-related proteins in mice with a high-fructose/high-fat diet. After the high-fructose/high-fat diet, the kidney expression levels of GLUT5, GLUT2, and SGLT2, were significantly increased compared to NC group, indicating increased renal reabsorption of fructose and glucose along with increased renal glucose output (Figs. 5a–5c). After intervention with allopurinol and 50 mg/kg

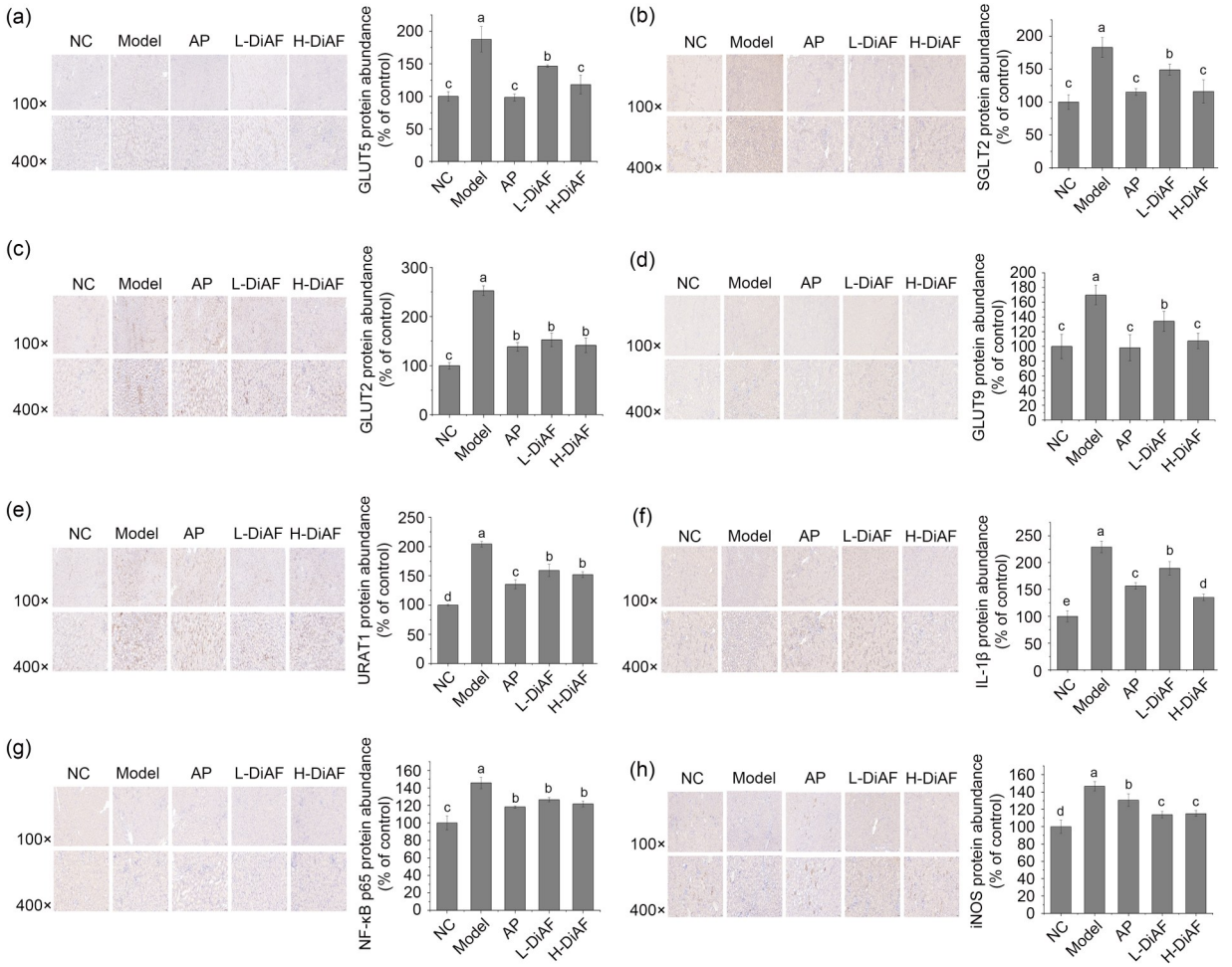

Fig. 5 IHC staining results and protein expression levels of GLUT5 (a), SGLT2 (b), GLUT2 (c), GLUT9 (d), URAT1 (e), IL-1β (f), NF-κB p65 (g), and iNOS (h) in the kidneys of mice. Values are expressed as mean±standard deviation (SD), *n*=10. Different letters marked above the bar indicate significant differences (*P*<0.05). IHC: immunohistochemistry; GLUT: glucose transporter; SGLT2: sodium-dependent glucose transporters 2; URAT1: urate transporter 1; IL-1β: interleukin-1β; NF-κB: nuclear factor-κB; iNOS: inducible nitric oxide synthase; NC: normal control; AP: positive; L-DiAF: low-dose diacylated anthocyanins from purple sweet potato (AF-PSPs); H-DiAF: high-dose diacylated AF-PSPs.

BW diacylated AF-PSPs, the expression levels of renal SGLT2 and GLUT5 in mice returned to normal levels, while GLUT2 expression showed a significant decrease. The low dose of diacylated AF-PSPs also led to a significant decrease in SGLT2, GLUT5, and GLUT2 expression levels. Allopurinol and diacylated AF-PSPs treatment modulated the renal reabsorption of fructose and glucose, and promoted renal fructose and glucose excretion. This helped to reduce renal burden and further reduced hyperglycemia in the mice. This result might be related to the effects of these treatments on lowering UA and regulating renal fructose metabolism. Similarly, the renal transporter proteins GLUT9 and URAT1 are the major renal UA reabsorption transporters for maintaining body homeostasis (Andres-Hernando, 2017). Inhibition of both might promote UA excretion, thereby restoring homeostasis of UA metabolism in the body. GLUT9 and URAT1 expression levels in the kidneys of mice in the Model group appeared significantly elevated compared to those of the NC group (Figs. 5d and 5e), indicating that feeding the mice with a high-fructose/high-fat diet for eight weeks resulted in increased renal reabsorption of UA and decreased renal UA excretion. In contrast, both allopurinol and diacylated AF-PSPs treatment significantly reduced the expression levels of GLUT9 and URAT1 in the kidneys of mice fed a high-fructose/high-fat diet. This indicated that the lowering of UA following treatment with allopurinol and diacylated AF-PSPs resulted in reduced UA reabsorption and increased UA excretion in the renal tubules of mice with metabolic syndrome, thereby reducing renal burden and correcting abnormal UA metabolism. This result is consistent with the modulation of mRNA levels of renal transport proteins by purple sweet potato extract in mice with hyperuricemia induced by potassium oxonate (Zhang ZC et al., 2019). This further indicates that diacylated AF-PSPs as an inhibitor of XO could not only inhibit hepatic UA production, but also reduce renal UA reabsorption and thus promote UA excretion in mice. This finally led to alleviation of the metabolic syndrome induced by the high-fructose/high-fat diet.

Both hyperglycemia and hyperuricemia can induce an inflammatory response leading to kidney injury. The activation of the NF-κB pathway is a key mechanism in the renal inflammatory response (Wang et al., 2015). NF-κB p65, IL-1β, and inducible nitric oxide synthase (iNOS) expression levels were significantly elevated in the kidneys of mice in the Model group compared to those in the NC group (Figs. 5f–5h), indicating that the metabolic syndrome caused inflammatory responses and kidney injury involving the NF-κB pathway in the kidneys. This was consistent with the results of renal pathology examination. After intervention with allopurinol and diacylated AF-PSPs, the expression levels of NF-κB p65, IL-1β, and iNOS in the kidneys of mice were significantly reduced compared to those of the Model group, indicating that the inflammatory response in the kidneys of mice was alleviated and the kidney injury caused by metabolic syndrome was mitigated to some extent. This effect might be related to the ability of diacylated AF-PSPs to inhibit renal *FK* expression and thus reduced ATP consumption during fructose phosphorylation. In this experiment, it was demonstrated that diacylated AF-PSPs could inhibit the renal inflammatory response and restore the normal morphological structure of the kidney in mice with metabolic syndrome induced by a high-fructose/high-fat diet. This might be related to the reduction of UA and regulation of *FK* expression in the fructose metabolic pathway of diacylated AF-PSPs. Diacylated AF-PSPs as a flavonoid with anti-inflammatory activity may have some advantages in alleviating kidney injury.

3.8 Human equivalent dose conversion based on body surface area

In this study, diacylated AF-PSPs at 50 mg/kg revealed promising hypouricemic activity, which might affect lipid metabolism to some extent and thus alleviated the symptoms of hyperglycemia in mice. Also, the modulation of renal function by diacylated AF-PSPs promoted the excretion of UA and glucose, showing a dual mechanism for alleviating hyperglycemia and hyperuricemia.

For prospective applications, it is highly recommended to identify the required dose of natural products when switching from one species to another, using the body surface area (BSA) normalization method (Reagan-Shaw et al., 2008). By calculating the true dose of diacylated AF-PSPs from mice to humans, we are able to assess an appropriate dose for clinical application and thus better explain its effect on improving hyperglycemia and hyperuricemia. Multiplying 50 mg/kg (mouse dose) by the K_m factor (3) for a mouse and then

dividing by the K_m factor (37) for a human results in a human equivalent dose for diacylated AF-PSPs of 4.05 mg/kg, which equates to a 243.24 mg dose of diacylated AF-PSPs for a 60-kg person. As the recommended daily intake of anthocyanins for humans ranges from 11.5 mg (in the USA) to 37.42 mg (in southern Europe) (Bars-Cortina et al., 2022), the maximum intake of anthocyanins should not exceed at most ten times its recommended level. This intake of 243.24 mg dose of diacylated AF-PSPs is within this range. This concentration might be achieved by taking a daily oral tablet, brewing using a lyophilized powder, or drinking a concentrate.

4 Conclusions

In this study we successfully established a hyperglycemia and hyperuricemia mice model induced by a high-fructose/high-fat diet. Diacylated AF-PSPs significantly improved the regulation of glucose metabolism. Intervention with diacylated AF-PSPs reduced weight gain, lowered blood UA values, and restored glucose tolerance in mice. In addition, the UA-lowering activity of diacylated AF-PSPs might also affect lipid metabolism and thus improve blood glucose regulation to some extent. The regulation of renal function further promotes UA and glucose excretion, achieving a dual regulation of hyperglycemia and hyperuricemia.

The hypouricemic effect of diacylated AF-PSPs as an XO inhibitor in mice was verified several times on a pre-laboratory basis. This study focused on discussing the alleviating effect of diacylated AF-PSPs on blood glucose in mice and the possible combination of the hypoglycemic and hypouricemic effects. On the one hand, diacylated AF-PSPs regulate the expression levels of the renal transporter proteins SGLT2, GLUT5, and GLUT2, decreasing the reabsorption of fructose and glucose and reducing renal glucose output. On the other hand, it reduces UA reabsorption and promotes UA excretion by moderating the expression levels of renal transporter proteins GLUT9 and URAT1, and also alleviates renal inflammation and restores the normal physiological structure and function of the kidney by inhibiting the renal NF-κB pathway and reducing IL-1β and iNOS expression.

This study revealed the linkage role in the occurrence and development of these two diseases, paving a key foundation and a feasible pathway for subsequent in-depth exploration of the relevant molecular mechanisms. We identified safe and effective dietary supplements suitable for the increasing number of patients with type 2 diabetes and hyperuricemia and some potential risk groups, and laid the pre-experimental and developmental foundations for the high-value utilization of AF-PSPs.

Acknowledgments

This work was supported by the National Key Technologies R&D Program of China (No. 2021YFE0194000) and the Fundamental Research Funds for the Central Universities of China (No. 2662018PY022).

Author contributions

Luhong SHEN: conceptualization, methodology, investigation, software, writing – original draft, paper revision, and experimental supplement. Yang YANG: methodology, resources, investigation, and software. Jiuliang ZHANG: writing – review & editing, project administration, and funding acquisition. Lanjie FENG: methodology and resources. Qing ZHOU: methodology and resources. All authors have read and approved the final manuscript, and therefore, have full access to all the data in the study and take responsibility for the integrity and security of the data.

Compliance with ethics guidelines

Luhong SHEN, Yang YANG, Jiuliang ZHANG, Lanjie FENG, and Qing ZHOU declare that they have no conflict of interest in this work.

Animal care including the room, cage, and equipment sanitation was in accordance with the standards for laboratory animals established by the People's Republic of China (GB14925-2010) and the 1964 Declaration of Helsinki Guiding Principles in the care and use of animals throughout the experimental period at the Center for Laboratory Animals, Huazhong Agricultural University (No. HZAUMO-2017-031). The animals were raised in a quiet environment with an appropriate temperature (25±1) °C and humidity (40±10)% and free access to water and food (No. SYXK(Hubei)2020-0084).

References

Adnan E, Rahman IA, Faridin HP, 2019. Relationship between insulin resistance, metabolic syndrome components and serum uric acid. *Diabetes Metab Syndr Chin Res Rev*, 13(3):2158-2162. https://doi.org/10.1016/j.dsx.2019.04.001

Adouni K, Zouaoui O, Chahdoura H, et al., 2018. *In vitro* antioxidant activity, α-glucosidase inhibitory potential and *in vivo* protective effect of *Asparagus stipularis* Forssk

aqueous extract against high-fructose diet-induced metabolic syndrome in rats. *J Funct Foods*, 47:521-530. https://doi.org/10.1016/j.jff.2018.06.006

Andres-Hernando A, Li NX, Cicerchi C, et al., 2017. Protective role of fructokinase blockade in the pathogenesis of acute kidney injury in mice. *Nat Commun*, 8:14181. https://doi.org/10.1038/ncomms14181

Bars-Cortina D, Sakhawat A, Piñol-Felis C, et al., 2022. Chemopreventive effects of anthocyanins on colorectal and breast cancer: a review. *Semin Cancer Biol*, 81:241-258. https://doi.org/10.1016/j.semcancer.2020.12.013

Gowd V, Karim N, Shishir MRI, et al., 2019. Dietary polyphenols to combat the metabolic diseases via altering gut microbiota. *Trends Food Sci Technol*, 93:81-93. https://doi.org/10.1016/j.tifs.2019.09.005

Hu QH, Zhang X, Pan Y, et al., 2012. Allopurinol, quercetin and rutin ameliorate renal NLRP3 inflammasome activation and lipid accumulation in fructose-fed rats. *Biochem Pharmacol*, 84(1):113-125. https://doi.org/10.1016/j.bcp.2012.03.005

Johnson RJ, Nakagawa T, Jalal D, et al., 2013. Uric acid and chronic kidney disease: which is chasing which? *Nephrol Dial Transplant*, 28(9):2221-2228. https://doi.org/10.1093/ndt/gft029

Jokioja J, Linderborg KM, Kortesniemi M, et al., 2020. Anthocyanin-rich extract from purple potatoes decreases postprandial glycemic response and affects inflammation markers in healthy men. *Food Chem*, 310:125797. https://doi.org/10.1016/j.foodchem.2019.125797

Khichar S, Choudhary S, Singh VB, et al., 2017. Serum uric acid level as a determinant of the metabolic syndrome: a case control study. *Diabetes Metab Syndr Chin Res Rev*, 11(1):19-23. https://doi.org/10.1016/j.dsx.2016.06.021

Kirakosyan A, Gutierrez E, Ramos-Solano B, et al., 2018. The inhibitory potential of Montmorency tart cherry on key enzymes relevant to type 2 diabetes and cardiovascular disease. *Food Chem*, 252:142-146. https://doi.org/10.1016/j.foodchem.2018.01.084

Krishnan E, Pandya BJ, Chung L, et al., 2012. Hyperuricemia in young adults and risk of insulin resistance, prediabetes, and diabetes: a 15-year follow-up study. *Am J Epidemiol*, 176(2):108-116. https://doi.org/10.1093/aje/kws002

Lu YL, Wu YM, Chen XF, et al., 2021. Water extract of *shepherd's purse* prevents high-fructose induced-liver injury by regulating glucolipid metabolism and gut microbiota. *Food Chem*, 342:128536. https://doi.org/10.1016/j.foodchem.2020.128536

Luo CL, Zhou Q, Yang ZW, et al., 2018. Evaluation of structure and bioprotective activity of key high molecular weight acylated anthocyanin compounds isolated from the purple sweet potato (*Ipomoea batatas* L. cultivar Eshu No.8). *Food Chem*, 241:23-31. https://doi.org/10.1016/j.foodchem.2017.08.073

Ma H, He K, Zhu JW, et al., 2019. The anti-hyperglycemia effects of *Rhizoma Coptidis* alkaloids: a systematic review of modern pharmacological studies of the traditional herbal medicine. *Fitoterapia*, 134:210-220. https://doi.org/10.1016/j.fitote.2019.03.003

Masarone M, Rosato V, Dallio M, et al., 2018. Role of oxidative stress in pathophysiology of nonalcoholic fatty liver disease. *Oxid Med Cell Longev*, 2018:9547613. https://doi.org/10.1155/2018/9547613

Nakagawa T, Johnson RJ, Andres-Hernando A, et al., 2020. Fructose production and metabolism in the kidney. *J Am Soc Nephrol*, 31(5):898-906. https://doi.org/10.1681/ASN.2019101015

Ng HY, Lee CT, Leung FF, et al., 2020. Effects of xanthine oxidase inhibitors and dapagliflozin on renal glucose and urate transporters in metabolic syndrome. *Nephrol Dial Transpl*, 35(S3):P0964. https://doi.org/10.1093/ndt/gfaa144.P0964

Nishikawa T, Nagata N, Shimakami T, et al., 2020. Xanthine oxidase inhibition attenuates insulin resistance and diet-induced steatohepatitis in mice. *Sci Rep*, 10:815. https://doi.org/10.1038/s41598-020-57784-3

Reagan-Shaw S, Nihal M, Ahmad N, 2008. Dose translation from animal to human studies revisited. *FASEB J*, 22(3):659-661. https://doi.org/10.1096/fj.07-9574LSF

Seo KH, Yokoyama W, Kim H, 2020. Comparison of polyphenol-rich wine grape seed flour-regulated fecal and blood microRNAs in high-fat, high-fructose diet-induced obese mice. *J Funct Foods*, 73:104147. https://doi.org/10.1016/j.jff.2020.104147

Spínola V, Llorent-Martínez EJ, Castilho PC, 2019. Polyphenols of *Myrica faya* inhibit key enzymes linked to type II diabetes and obesity and formation of advanced glycation end-products (*in vitro*): potential role in the prevention of diabetic complications. *Food Res Int*, 116:1229-1238. https://doi.org/10.1016/j.foodres.2018.10.010

Thongnak L, Chatsudthipong V, Lungkaphin A, 2020. Mitigation of renal inflammation and endoplasmic reticulum stress by vildagliptin and statins in high-fat high-fructose diet-induced insulin resistance and renal injury in rats. *Biochim Biophys Acta Mol Cell Biol Lipids*, 1865(9):158755. https://doi.org/10.1016/j.bbalip.2020.158755

van Hung T, Wanatanbe J, Yonejima Y, et al., 2019. Exopolysaccharides from *Leuconostoc mesenteroides* attenuate chronic kidney disease in mice by protecting the intestinal barrier. *J Funct Foods*, 52:276-283. https://doi.org/10.1016/j.jff.2018.11.005

Vilà L, Rebollo A, Ađalsteisson GS, et al., 2011. Reduction of liver fructokinase expression and improved hepatic inflammation and metabolism in liquid fructose-fed rats after atorvastatin treatment. *Toxicol Appl Pharmacol*, 251(1):32-40.

https://doi.org/10.1016/j.taap.2010.11.011

Wang L, Zhao Y, Zhou Q, et al., 2017. Characterization and hepatoprotective activity of anthocyanins from purple sweet potato (*Ipomoea batatas* L. cultivar *Eshu* No. 8). *J Food Drug Anal*, 25(3):607-618. https://doi.org/10.1016/j.jfda.2016.10.009

Wang MX, Liu YL, Yang Y, et al., 2015. Nuciferine restores potassium oxonate-induced hyperuricemia and kidney inflammation in mice. *Eur J Pharmacol*, 747:59-70. https://doi.org/10.1016/j.ejphar.2014.11.035

Wang YJ, Zheng YL, Lu J, et al., 2010. Purple sweet potato color suppresses lipopolysaccharide-induced acute inflammatory response in mouse brain. *Neurochem Int*, 56(3): 424-430. https://doi.org/10.1016/j.neuint.2009.11.016

Yang Y, Zhang ZC, Zhou Q, et al., 2020a. Hypouricemic effect in hyperuricemic mice and xanthine oxidase inhibitory mechanism of dietary anthocyanins from purple sweet potato (*Ipomoea batatas* L.). *J Funct Foods*, 73:104151. https://doi.org/10.1016/j.jff.2020.104151

Yang Y, Zhang JL, Zhou Q, 2020b. Targets and mechanisms of dietary anthocyanins to combat hyperglycemia and hyperuricemia: a comprehensive review. *Crit Rev Food Sci Nutr*, 62(4):1119-1143. https://doi.org/10.1080/10408398.2020.1835819

Zhang JT, Sun LJ, Dong YS, et al., 2019. Chemical compositions and α-glucosidase inhibitory effects of anthocyanidins from blueberry, blackcurrant and blue honeysuckle fruits. *Food Chem*, 299:125102. https://doi.org/10.1016/j.foodchem.2019.125102

Zhang QY, Pan Y, Wang R, et al., 2014. Quercetin inhibits AMPK/TXNIP activation and reduces inflammatory lesions to improve insulin signaling defect in the hypothalamus of high fructose-fed rats. *J Nutr Biochem*, 25(4):420-428. https://doi.org/10.1016/j.jnutbio.2013.11.014

Zhang ZC, Su GH, Luo CL, et al., 2015. Effects of anthocyanins from purple sweet potato (*Ipomoea batatas* L. cultivar Eshu No.8) on the serum uric acid level and xanthine oxidase activity in hyperuricemic mice. *Food Funct*, 6(9): 3045-3055. https://doi.org/10.1039/C5FO00499C

Zhang ZC, Zhou Q, Yang Y, et al., 2019. Highly acylated anthocyanins from purple sweet potato (*Ipomoea batatas* L.) alleviate hyperuricemia and kidney inflammation in hyperuricemic mice: possible attenuation effects on allopurinol. *J Agric Food Chem*, 67(22):6202-6211. https://doi.org/10.1021/acs.jafc.9b01810

Supplementary information

Tables S1 and S2; Fig. S1